Available online at www.sciencedirect.com
ScienceDirect
Journal of Luminescence 126 (2007) 353–358
JOURNAL OF LUMINESCENCE
www.elsevier.com/locate/jlumin

$Y_2O_2S:Eu^{3+}$ nanocrystals, a strong quantum-confined luminescent system

J. Thirumalai, R. Jagannathan*, D.C. Trivedi

Luminescence Group, Central Electro Chemical Research Institute, Karaikudi 630 006, Tamil Nadu, India

Received 23 January 2006; received in revised form 1 August 2006; accepted 9 August 2006
Available online 25 September 2006

Abstract

Trivalent europium-doped yttrium oxysulfide nanocrystals synthesized using sol–gel thermolysis show significant blue shifts in the excitation bands corresponding to fundamental absorption, charge-transfer absorption. A significant blue shift observed in the fundamental absorption edge for the nanocrystals having an average crystallite size (ϕ) in the range 9–15 nm indicates a strong quantum confinement with a Bohr exciton radius of 5–13 nm. Also, the diffuse reflectance spectra and the corresponding Kubelka–Munk plot indicate the possibility of profound decrease in the absorption coefficient of Eu^{3+}–ligand charge-transfer species necessitating further studies in this wide-gap semiconductor nanocrystalline system.

Keywords: Nanocrystals; Oxysulfide; Photoluminescence; Quantum confinement; Europium

1. Introduction

Trivalent-europium-doped yttrium oxysulfide ($Y_2O_2S:Eu^{3+}$) is an important phosphor system extensively applied in color-television picture tubes and, of late, in field-emission display devices [1,2]. Yttrium oxysulfide, with a bandgap of 4.6–4.8 eV can be considered as a large bandgap semiconductor system [3]. Hence, size miniaturization of this system may be fascinating as it can lead to quantum structures. Recently, we reported the synthesis of $Y_2O_2S:Eu^{3+}$ nanocrystals through *sol–gel* thermolysis in one or two steps employing different organic precursors [4,5]. In these preliminary studies reporting the syntheses of this new naocrystalline system, we carried out optical studies related to spectral shift observed in the photoluminescence excitation (PLE) band(s) corresponding to fundamental absorption and europium–ligand charge-transfer band (CTB) regions which made possible to have rough idea on the spectral shift and allied features. With an objective of making a precise and thorough spectral study on this new nanocrystalline system, we extended the investigation using diffuse reflectance spectra and also the Kubelka–Munk plot. From this we have that the fundamental absorption edge of this semiconductor nanocrystalline system shows significant blue shift of about 0.29 ± 0.01 eV. This seems to suggest a strong quantum confinement effect [6,7]. It is significant to note that recently there are several reports on size-dependent blue shift in the fundamental absorption edge which enable to predict opto-electronic properties of various nanocrystalline samples [8,9]. Since nanocrystals of this wide-gap semiconductor system may have potential for application, we are motivated to analyze the results in more detail.

2. Experimental

In this study, Eu^{3+}-doped yttrium-oxysulfide nanocrystals were synthesized using a two-step sol–gel polymer thermolysis method and characterized as described before [4,5]. The method of synthesis essentially comprises in first synthesizing Eu^{3+}-doped yttrium-oxide nanocrystals followed by sulfurization in the second stage. Size tunability to have a controlled size of the target oxysulfide nanocrystals was achieved by controlling concentration ratio between the reactant lanthanide metallic nitrate(s) to

*Corresponding author.
E-mail address: jags57_99@yahoo.com (R. Jagannathan).

0022-2313/$ - see front matter © 2006 Elsevier B.V. All rights reserved.
doi:10.1016/j.jlumin.2006.08.064

organic polymeric networks with the latter acting as fuel-cum-dispersion medium.

All the chemicals used in this synthesis were either analyzed reagents or were better than 99.9% purity. In this study, all samples (bulk and nanocrystalline) had the same concentration of europium at 2 mol% with respect to yttrium content in Y_2O_2S. The thermolysis product was found to contain the target $Y_2O_2S{:}Eu^{3+}$ nanocrystalline phase and also a secondary phase due to sodium polysulfide Na_2S_x ($x = 4$) as flux residue. But the latter, impurity phase could be effectively removed through water washing. All measurements such as diffuse reflectance, photoluminescence, X-ray powder diffraction (XRD), etc., were done within the first few hours of the sample synthesis. In this investigation, we present the spectral properties of nanoparticles of two sizes labeled as B and C respectively having mean crystallite sizes of 15 and 9 nm and are compared with polycrystalline bulk sample (labeled as sample A) having an average particle size of 0.5 μm as determined using scanning electron microscopy (SEM).

3. Results and discussion

Crystallographic unit-cell parameter values obtained from the XRD data, and refined using a standard least-squares refinement procedure are in good agreement with standard JCPDS # 24-1424 values corresponding to the polycrystalline Y_2O_2S phase (Fig. 1 and Table 1). In the case of nanocrystalline sample(s), there is a marginal decrease (~0.3%) in unit-cell volume which can be attributed to cell contraction owing to an increase in the surface area of the crystallites [10].

As can be seen from the SEM image given in Fig. 2a, the polycrystalline bulk sample shows a hexad morphology consistent with $P\bar{3}ml$ crystal structure with an average particle size of 0.5 μm. However, in the case of nanocrystals, as can be seen from the transmission electron microscope image of the thermolysis product corresponding to the oxysulfide nanocrystals (Fig. 2b), the particles are slightly agglomerated to make out precise morphology impossible. Furthermore, the selected-area electron diffraction (SAED) pattern obtained for the nanosample (Fig. 2c) is in good agreement with the XRD pattern corresponding to the target Y_2O_2S phase confirming the oxysulfide phase of the material investigated.

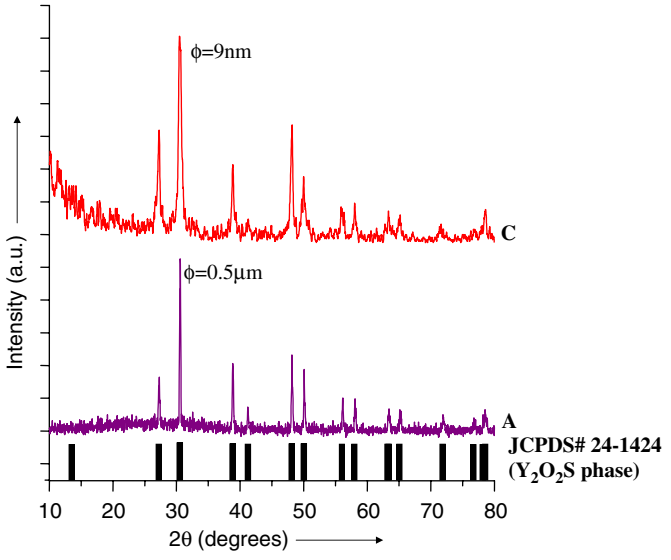

Fig. 1. XRD patterns (using CuK_α; $T = 300$ K) of bulk (A) and nanocrystalline (C) $Y_2O_2S{:}Eu^{3+}$(2%) samples.

Table 1
Least-squares refined crystallographic cell parameters for bulk and nanocrystalline $Y_2O_2S{:}Eu^{3+}$ samples (space group $P\bar{3}ml$)

Sample (size ϕ)	Crystallographic cell parameters			Cell volume (Å)^3
	$a = b$ (Å)	c (Å)	c/a	
Standard—JCPDS # 24-1424	3.784	6.589	1.741	81.710
A (0.5 μm)	3.784	6.589	1.742	81.691
B (15 nm)	3.782	6.586	1.740	81.510
C (9 nm)	3.780	6.581	1.741	81.440

The diffuse reflectance spectrum (Fig. 3a) corresponding to the bulk sample (sample A) shows two bands around 260 and 290 nm corresponding to fundamental absorption of the oxysulfide host and the Eu^{3+}–X^{2-}(ligand X = O/S) charge-transfer excitation regions. These bands were separately fitted as individual Gaussian bands and are given in the insets of Fig. 3. From this, it can be seen that the fundamental absorption edge of nanocrystalline oxysulfide host shows a blue shift of about 2000–2400 cm^{-1} (0.24–0.295 eV) and also the CTB shows a blue shift of 2400 cm^{-1} (0.3 eV for sample B) with respect to the bulk sample. The blue shift observed in the fundamental absorption edge of the nanocrystalline oxysulfide host can be rationalized by considering quantum confinement effect in this wide-gap semiconductor system. The blue shift observed in the fundamental absorption edge corresponds to an enhancement in the bandgap value $\Delta E_g = 0.295$ eV for the nanocrystalline oxysulfide system with respect to the bulk counterpart. The reduced electron effective mass determined [6] using the knowledge of the blue shift (ΔE_g) is

$$(\Delta E_g) = \hbar^2\pi^2/2\mu\phi^2. \quad (1)$$

This gets a reduced effective mass value (μ) of $0.01m_e$ for sample C. Applying this value in the equation [7]:

$$a_B = \hbar^2\varepsilon/e^2\mu, \quad (2)$$

we can get the value of exciton Bohr radius for this quantum structure (Table 2). In the present study, we get a Bohr exciton radius (a_B) value of 5.3 nm using the value of low-frequency (static) and high-frequency (optical) dielectric constants $\varepsilon = 12.51$ or 5.23 given by Mikami

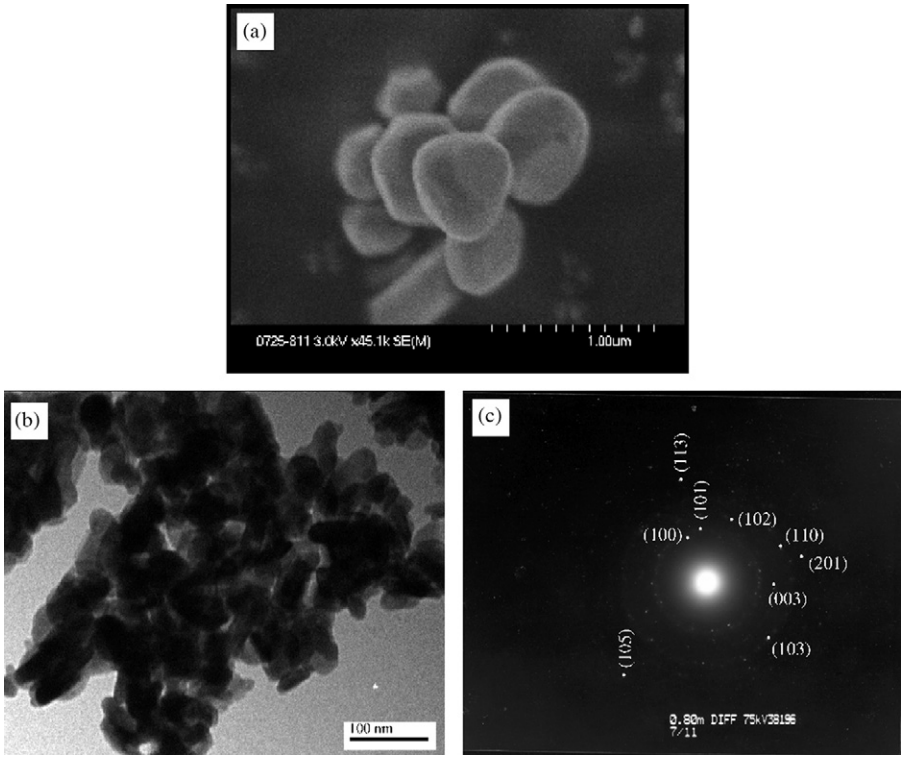

Fig. 2. (a) Scanning electron microscope image (for bulk sample-A) and (b) transmission electron microscope image for nanocrystalline $Y_2O_2S:Eu^{3+}$ sample (for sample-C) and (c) the corresponding SAED pattern.

et al. in Ref. [11]. The value of a_B determined for this semiconductor nanocrystalline system being nearly comparable to the crystallite size may lead to nearly strong quantum confinement in the present case [6,7]. For reasons of completion, we compare the results of the new quantum system with results of other established systems available from literature [7,12–14] as presented in Table 3. Form this comparison, we have that the new system holds a good comparison with CdS system in terms of blue shift in the absorption edge and exciton size estimated from there. Not withstanding this, in many other quantum systems there are many differences in the blue shift vis a vis exciton size, which in our opinion may be due to other parameters involved in the calculation such as dielectric constant(s) of the system under study and other parameters. Hence this merits further detailed studies along these lines which will be our future goal.

Furthermore, it should be noted that between bulk and nanosamples, the difference in reflectance values corresponding to the fundamental absorption band is marginal which may not be of any practical significance. On the other hand, it is possible to observe a substantial decrease in the reflectance corresponding to the CTB region. Hence in an attempt to have a deeper insight on this behavior, we plotted the corresponding Kubelka–Munk plot for these reflectance curves as presented in Fig. 4.

Kubelka–Munk function also called as remission function $F(R)$ is given by

$$F(R) = (1 - R)^2/2R = k/s = Ac/s \quad (3)$$

with R, A, k, s and c being reflectance, absorbance, absorption coefficient, scattering coefficient and concentration of the absorbing species, respectively.

Accordingly, the remission function $F(R)$ values for the bulk and the nanosamples at spectral regions related to both the fundamental and charge-transfer absorption band(s) were calculated as given in Table 2. This may indicate a possibility of significant decrease in remission function in the case of nanocrystalline system for the region corresponding to the CTB region when compared with that of the fundamental absorption. This may suggest a significant decrease in the concentration of absorbing species/absorption coefficient corresponding to $Eu^{3+} \leftrightarrow \rightarrow$ ligand charge-transfer transition resulting from possible change in optical electronegativities of species (Eu^{3+}/X^{2-}) involved. However it should be noted that the scattering factors for bulk and nanosamples need not be the same and even a small difference in the reflectance value(s) can be crucial to influence the absorption coefficient in this region. Hence detailed studies are necessary to draw precise conclusions on the change in absorption coefficient due to size reduction in this luminescent system.

Now turning to explain the blue shift in the Eu^{3+}–ligand CTB: since it is not possible to precisely ascertain the position of the CTB (v_{ct}) for the 9 nm particles (sample C), we take into consideration the CTB for the 15 nm particles (sample B) which show a blue shift of about 2420 cm^{-1} with respect to the bulk sample. This blue shift implies an enhancement in optical electronegativity. From the Jorgensen's empirical relation [15] correlating optical

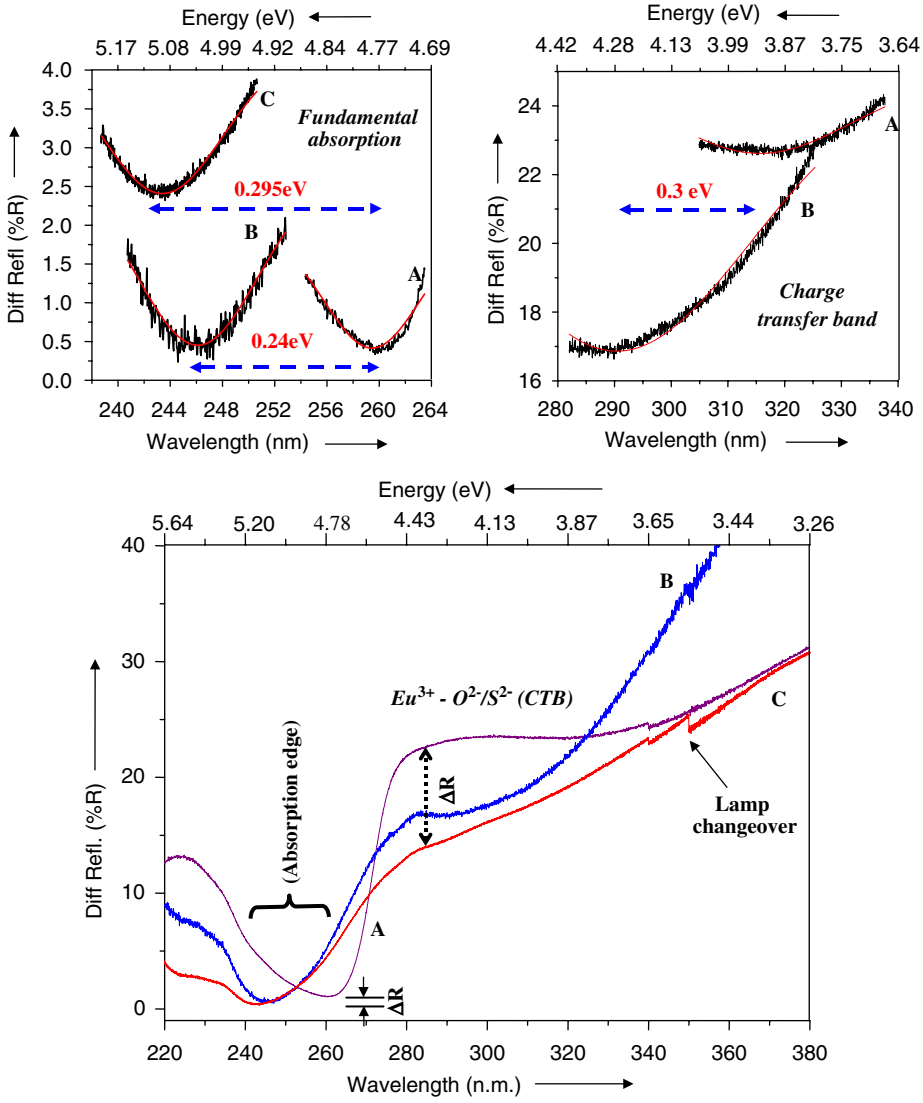

Fig. 3. (a) Diffuse reflectance spectra of bulk (A) and nanocrystalline (B, C) $Y_2O_2S:Eu^{3+}$ samples. ΔR and $\Delta R'$ are differences in the reflectance values corresponding to fundamental absorption and charge-transfer band regions, respectively. Inset: Gaussian fits for fundamental absorption and charge-transfer bands of bulk and nanosamples. The spectral shifts are indicated in eV.

Table 2
Some optical data on Eu^{3+}(2%)-doped Y_2O_2S nanocrystals

Sample (size)	Spectral data									
	From fundamental absorption (excitonic) band						From charge transfer band			
	Diffuse reflectance		Abs. edge (cm^{-1})	Reduced electron effective mass (μ)	Bohr radius a_B (nm)		λ_{max} (cm^{-1})	$\Delta\chi^*$ (± 0.01)	Diffuse reflectance	
	R (%)	$F(R)$			$\varepsilon_{\alpha\alpha}^{\infty}$	$\varepsilon_{\alpha\alpha}^{0}$			R (%)	$F(R)$
A (0.5 μm)	0.954	0.8253	38 759	—	—	—	31 696	1.29	22.2	13.7
B (15 nm)	0.696	0.5679	40 700	$0.004m_e$	5.5	13.2	34 352	1.35	17.0	12.3
C (9 nm)	0.675	0.5468	41 138	$0.01m_e$	2.2	5.3	34 435	1.38	13.7	10.2

electronegativity and lanthanide–ligand CTB, we have that the position of the CTB given by

$$\nu_{ct} = [\chi_{opt}(X) - \chi_{uncorr}(Eu^{3+})] \times 30,000\,cm^{-1} \quad (4)$$

with $\chi_{opt}(X)$ and χ_{uncorr} (Eu^{3+}) being the optical electronegativities of the ligand(s) and the Eu^{3+} ion, respectively. This may suggest either an increase in $\chi_{opt}(X)$, the optical electronegativity of the ligand(s), or a decrease in χ_{uncorr}

Table 3
Blue shift vis-à-vis exciton size in several quantum structures

System	Crystallite size ϕ (in nm)	Bandgap (in eV)	Shift in bandgap ΔE_g (in eV)	Bohr exciton radius a_B (in nm)	References
$Y_2O_2S:Eu^{3+}$	9	4.6–4.8	0.295	5.3	Our work
CdSe	1.4	1.74	1	4.8	Jungnickel et al. [7]
CdS	4.9	2.58	0.185	5	White et al. [12]
ZnO	3–4	3.44	0.23	1.25	Li et al. [13]
ZnS	2.5	3.6	0.59	1.1	Vogel et al. [14]

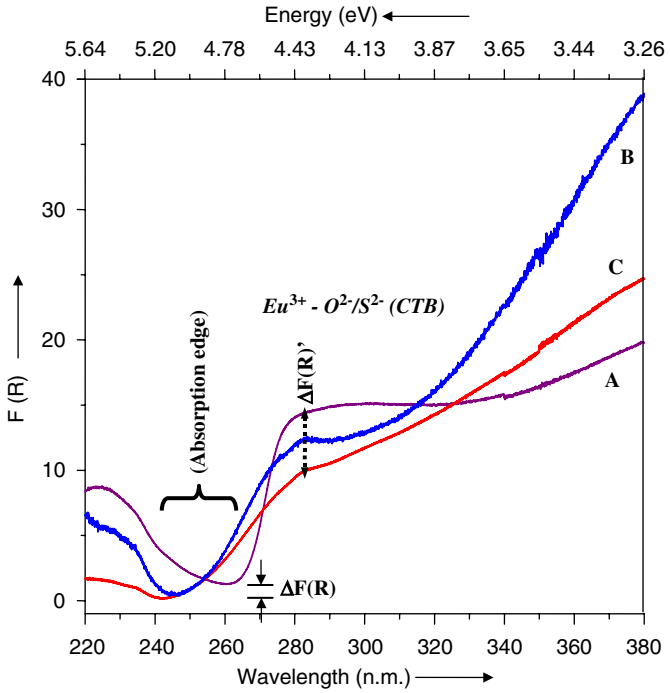

Fig. 4. Kubelka–Munk plot for bulk (A) and nanocrystalline (B, C) $Y_2O_2S:Eu^{3+}$ samples.

(Eu^{3+}), the optical electronegativity of the central Eu^{3+} ion. Increase in (optical) electronegativity for the ligand(s)/anions means increase in ionicity (decrease in covalency). This will translate into higher energy for facilitating the Eu^{3+}–$X^{2-}(4f^7 2p^{-1})$ ligand-to-metal electron (charge) transfer transition. The electron configuration $4f^7 2p^{-1}$ related to Eu–ligand CTB refers to a reduction reaction where one p electron from the ligand is transferred to europium ion resulting in the reduction of europium from Eu^{3+} to Eu^{2+} [16].

Furthermore, we have from the Duffy relation [17] connecting the change in optical electronegativity to the bandgap (E_g) of the host system that change in optical electronegativity

$$\Delta\chi^* = 0.2688E_g. \quad (5)$$

Hence, an increase in the bandgap value by 0.30 eV for the nanocrystalline system implies an increase in the optical electronegativity difference ($\Delta\chi^*$) by 0.09 ± 0.01. In any case, the increase in optical electronegativity cannot be assigned to the Eu^{3+} ion involving inner shell f-electrons. Instead, it can be attributed to the ligand(s) surrounding the Eu^{3+} ion. It seems possible that surface states (SS) generated from broken, truncated chemical bonds and the lack of long-range lattice order may be some possible cause(s) for this situation.

It is known that the Eu^{3+}–ligand charge-transfer transition and the related processes can be described by a configurational–coordinate (c–c) model. The electron configuration of the Eu^{3+}–ligand charge-transfer state will correspond to the electron configuration $4f^7 2p^{-1}$ of the europium ion. This means that one p-electron from the ligand will be transferred to Eu^{3+} ion converting it to Eu^{2+} and a free hole. In a covalent system like $Y_2O_2S:Eu^{3+}$, it is reasonable that the charge-transfer-state can as well be considered as an Eu^{3+} center plus an electron–hole pair. This means that the present situation can be described by an exciton attached to Eu^{3+} impurity center.

On the other hand, turning to photoluminescence emission spectra, it should be mentioned that within the spectral resolution of our experimental set-up, we could not observe any substantial difference in the Stark-splitting spectral pattern for various $^5D_0 \rightarrow {}^7F_J$ emission components between bulk and nanosamples (Stark-splitting pattern consistent with C_{3v} point group symmetry for Y^{3+}/Eu^{3+} cationic sites in these cases, Fig. 5b). Hence it seems reasonable to predict similar chemical surroundings for the bulk and nanocrystalline samples. Notwithstanding nearly comparable Stark-splitting pattern of Eu^{3+} levels in the bulk and nanosample, a significant difference can be noticed on the hyper-sensitive $^5D_0 \rightarrow {}^7F_2$ transition of Eu^{3+}. For the nanocrystalline sample, of the two lines in this transition observed at 615 and 626 nm, the latter gains considerable intensity against the former. Although it is not possible to explain this feature precisely, one explanation that seems to merit consideration would be the possibility of non-radiative resonant energy transfer to Eu^{3+} in yttrium oxide crystallites. It has been experimentally established that the formation of yttrium oxysulfide particles takes place over yttrium oxide nuclei [18]. Furthermore, the dominant $^5D_0 \rightarrow {}^7F_2$ luminescent transition of yttrium oxide lying around 611 nm is closer to the 615 nm Stark component of YOS which might eventually render intense emission at 615 nm from YOS nanoparticles impossible.

Now turning to compare the PLE spectra (Fig. 5a), it can be seen that the weak fine structure due to direct f–f excitation lines of Eu^{3+} centers observed in the bulk system (sample A) are absent in the nanocrystalline sample (sample C). This may

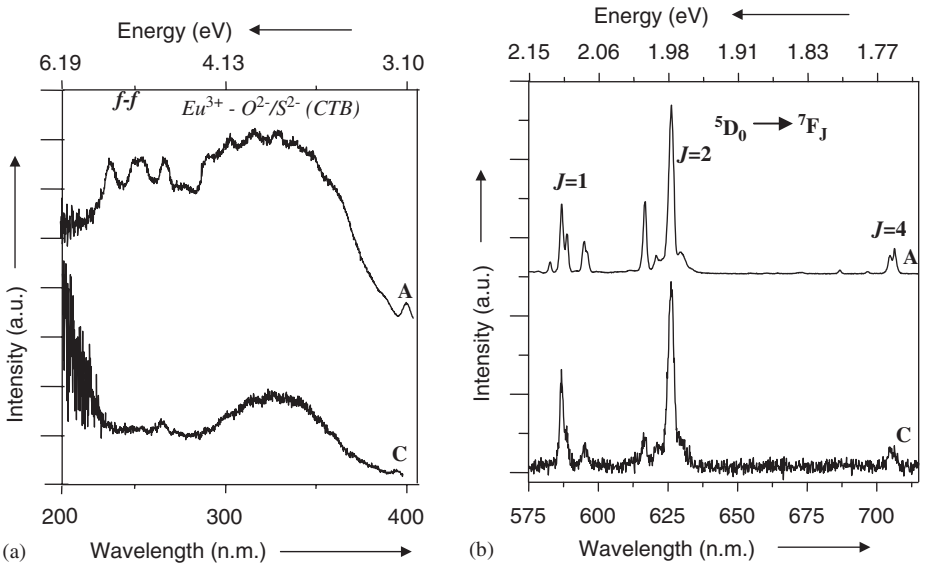

Fig. 5. (a) Photoluminescence excitation spectra monitoring $^5D_0 \rightarrow {}^7F_2$ emission in Eu^{3+} in ($\lambda_{em} = 626$ nm) bulk (sample A) and nanocrystalline (sample C) oxysulfide samples. f–f indicate Eu^{3+} direct excitation lines. (b) Photoluminescence emission spectra ($\lambda_{exc} = 320$ nm) corresponding to various $^5D_0 \rightarrow {}^7F_J$ ($J = 1, 2, 4$) transitions revealing identical Stark-splitting patterns for both bulk (A) and (C) nanosamples.

be due to a pronounced interaction between f–f levels of the Eu^{3+} dopant and the blue-shifted fundamental absorption edge of the nanocrystalline YOS host matrix.

4. Conclusions

In summary, luminescence properties of Eu^{3+} in Y_2O_2S nanocrystals ($\phi = 9$–15 nm) showed significant blue shifts both in the fundamental absorption edge and in Eu^{3+}–X^{2-} (ligand X = O/S) charge-transfer (excitation) bands. These respectively signify a strong quantum confinement and possibility of an increase in the difference in optical electronegativities. Optical reflectance data indicate a possibility of significant decrease in the absorption coefficient corresponding to Eu^{3+}–X^{2-} (ligands) charge-transfer region warranting further detailed studies in this direction.

References

[1] M.R. Royce, US Patent no. 3418, vol. 246, 1968.
[2] S.H. Cho, Y.S. Yoo, J.D. Lee, J. Electrochem. Soc. 145 (1998) 1017.
[3] M. Mikami, A. Oshiyama, Phys. Rev. B 57 (1998) 8939.
[4] J. Dhanaraj, R. Jagannathan, D.C. Trivedi, J. Mater. Chem. 13 (2003) 1778.
[5] J. Dhanaraj, M. Geethalakshmi, R. Jagannathan, T.R.N. Kutty, Chem. Phys. Lett. 387 (2004) 23.
[6] L.E. Brus, J. Chem. Phys. 79 (1983) 5566.
[7] V. Jungnickel, F. Henneberger, J. Lumin. 70 (1996) 238.
[8] R. Viswanatha, S. Sapra, B. Satpati, P.V. Satyam, B.N. Dev, D.D. Sarma, J. Mater. Chem. 14 (2004) 661.
[9] B. Mercier, C. Dujardin, G. Ledoux, C. Louis, O. Tillement, J. Appl. Phys. 96 (2004) 650.
[10] Q. Li, L. Go, D. Yan, Mater. Chem. Phys. 64 (2000) 41.
[11] M. Mikami, S. Nakamura, M. Itoh, Phys. Rev. B 65 (2002) 094302.
[12] C.W. White, A. Meldrum, J.D. Budai, S.P. Withrow, E. Sonder, R.A. Zuhr, D.M. Hembree Jr., M. Wu, D.O. Henderson, Nucl. Instrum. Methods B 148 (1999) 991.
[13] C. Li, S. Xiyu, W. Zhenyu, Z. Bingsuo, D. Jiahua, X. Sishen, Chem. J. Int. 4 (2002) 45.
[14] W. Vogel, P.H. Borse, N. Deshmukh, S.K. Kulkarni, Langmuir 16 (2000) 2032.
[15] C.K. Jorgensen, Prog. Inorg. Chem. 12 (1970) 101.
[16] C.A. Kodairaa, H.F. Britoa, O.L. Malta, O.A. Serra, J. Lumin. 101 (2003) 11.
[17] J.A. Duffy, Physica C 13 (1980) 2979.
[18] L. Ozawa, J. Electrochem. Soc. 124 (1970) 413.